

# Melt-mineral-fluid interaction in peralkaline silicic intrusions in the Oslo Rift, Southeast Norway.

## II. High-temperature fluid inclusions in the Eikeren-Skrim complex

THOR H. HANSTEEN & ERNST A.J. BURKE.

Hansteen, T.H. & Burke, E.A.J. 1990: Melt-mineral-fluid interaction in peralkaline silicic intrusions in the Oslo Rift, Southeast Norway. II. High-temperature fluid inclusions in the Eikeren-Skrim complex. *Nor. Geol. Unders. Bull.* 417, 15-32.

The Eikeren-Skrim subvolcanic granite complex consists of mildly peralkaline rocks, most of which contain abundant miarolitic cavities. Optical microscope studies reveal that several generations of fluids and solids were trapped in rock-forming (magmatic) and miarolitic quartz. A fluid evolution history has been worked out, involving (1) magmatic, (2) submagmatic (i.e. sub-solidus fluids possessing the chemical characteristics of the magmatic fluids) and (3) post-magmatic fluids. Combined energy dispersive analyses and laser Raman microprobe studies were used for the identification of daughter minerals. Primary magmatic inclusions comprise single mineral grains, grain clusters ( $\pm$  glass) (interpreted as crystallized samples of silicate melts), and high-salinity fluid inclusions, which are best described as hydrosaline melts. Optical estimates of phase ratios between vapour, liquid and identified solids in fluid inclusions show high concentrations of Cl, S, Na, K, Ca (and possibly Fe) in the magmatic and submagmatic fluids. Early post-magmatic fluids were mainly characterized by high Cl, Na and K contents, and represent a change in fluid regime from sulphur-rich and highly peralkaline to alkali chloride dominated. Post-magmatic fluids were gradually diluted through mixing with meteoric water.

*T.H. Hansteen, Mineralogisk-Geologisk Museum, Sars Gate 1, N-0562 Oslo 5, Norway.*

*E.A.J. Burke, Vrije Universiteit, Instituut voor Aardwetenschappen, postbus 7161, 1007 MC Amsterdam, The Netherlands.*

### Introduction

The compositions and quantities of fluids dissolved in silicate melts have important consequences for solidus temperatures and stabilities of magmatic minerals, as well as for ore-forming processes (e.g. Burnham 1979). Post-magmatic fluid evolution has implications for the final mineral assemblages in plutonic rocks (Orville 1963, Roedder 1971, Lagache & Weissbrod 1977). Fluid inclusions in minerals are the only samples available of original fluids which interacted with a rock at specific points in its P-T-x evolution (x is chemistry). Thus, the different fluid inclusion generations in a granitic rock may contain information on magmatic fluids which exsolved upon solidification, as well as on fluids that interacted with solid mineral phases during post-magmatic conditions.

This study establishes the fluid and solid inclusion chronology in the Eikeren-Skrim peralkaline granite complex (ESG; see Fig. 1), and provides an estimate of the chemical com-

position of the earliest fluid inclusion generations in the complex. Microthermometric studies are treated separately (Hansteen 1988 and in prep.).

### Geological setting

Ekerites in the Permian Oslo Rift are the granitic end-members in a series of alkali syenitic (nordmarkite) to peralkaline granitic rocks (Barth 1945, Neumann 1976, Neumann et al. 1977, Neumann et al. 1990). (Discussions on the provenance of the alkaline Oslo Rift magmas have been summarized by Neumann et al. 1988 and Rasmussen et al. 1988.) In the field, ekerite occurs as intrusions with sharp contacts, and as masses with gradational contacts to nordmarkite (Brøgger 1906, Barth 1945, Sæther 1962, Dietrich et al. 1965). Rb-Sr studies (Sundvoll 1978, Rasmussen et al. 1988) show that the ekerite complexes are among the youngest plutonic rocks in the Oslo Paleorift. Dietrich et al. (1965) suggested

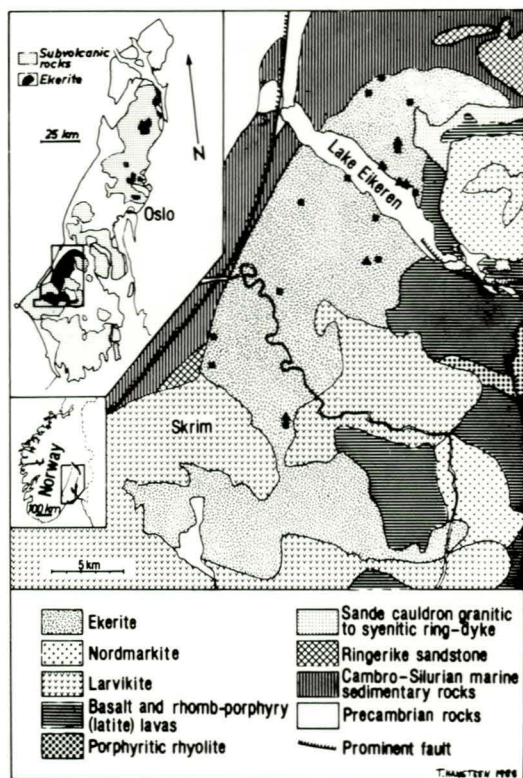


Fig. 1: Geological map of the Eikeren-Skrim granite complex (ESG) and its immediate surroundings. The map is compiled mainly from Ramberg (1976), Brøgger & Schetelig (1926), Raade (1973 and unpubl.), Andersen (1981) and Brink Larsen & Kristensen (unpubl.). Localities for selected fluid inclusion samples are marked with squares for rock-forming quartz, and triangles for quartz from miarolitic cavities. Inset: schematic outline of the Oslo Paleorift, showing the areal extent of the subvolcanic rocks (stippled) and ekerite (black).

that late-magmatic fluid ('volatile') transfer processes could explain some anomalously low but quite variable trace element concentrations peculiar to ekerite. This idea was supported by Raade (1973), and partially by Neumann (1976) and Neumann et al. (1977). On the basis of variable and comparatively high Th/U ratios, and high but variable  $^{87}\text{Sr}/^{86}\text{Sr}$  initial ratios (Heier & Compston 1969), Raade (1973, 1978) concluded that the ekerite magmas had been subject to processes in addition to closed system fractionation. He proposed high-level fractionation combined with U loss, crustal contamination and fluid transfer as likely mechanisms. Rasmussen et al. (1988) and Neumann et al. (1990) showed that late-stage

processes involving a fluid phase were indeed important for the trace element characteristics of these rocks.

The ESG is part of the Oslo Region Permian subvolcanic batholith complex, which comprises monzonitic to syenitic (larvikites), alkali syenitic (nordmarkites) and alkali granitic rocks (ekerites and biotite granites). Rb-Sr whole-rock dating gives an age of  $271 \pm 2$  Ma (Rasmussen et al. 1988). The ESG is the most voluminous peralkaline granite in the Oslo Paleorift. Gravity studies reveal a mushroom-shaped body reaching a depth of at least 7 km below the present surface (Ramberg 1976). To the south, the ESG intrudes older Permian larvikites, rhomb-porphry lavas (latites) and basalts. On the eastern side, it is bordered by the igneous rocks of the Sande caudron. To the north and west, the ESG cuts a sequence of Cambro-Silurian interbedded shales and limestones. The northern part of the complex is the type area for ekerite (Brøgger 1890, 1906).

## Petrography

The rock type ekerite was originally described as an alkali granite, usually characterized by the presence of alkali amphibole, with ægirine as a commonly occurring mineral (Brøgger 1906). Oftedahl (1948) defined ekerite as alkali granite without plagioclase, consisting mainly of perthitic feldspar, quartz, ægirine and/or alkali amphibole. Amphibole is present in all investigated types in the ESG, and discrete plagioclase grains are uncommon.

The main rock type in the ESG is a hypidiomorphic to allotriomorphic, dominantly equigranular granite, typically containing 20 to 30 volume percent quartz and 60 to 80 percent dominantly mesoperthitic feldspar. The normal grain diameters of the felsic minerals are 2 to 15 mm. Perthite grains are generally covered by a thin rim of albite. A few samples contain late, separate albite grains in subordinate amounts.

Amphiboles comprise 1 to 10 % of the rock. Samples analysed by Neumann (1976) and Neumann et al. (1990) classify as manganoan arfvedsonites and manganoan magnesioarfvedsonites to richterites (Leake 1978). All amphiboles are F-rich. Most samples also contain acmitic pyroxene (0-20 %). The opaque phases (0.5-5 %) are magnetite and members of the series ilmenite-pyrophanite (Neu-

mann 1974). Apatite, zircon and most commonly also sphene occur in minor amounts. Rutile, fluorite, biotite, pyrite, astrophyllite and elpidite (the last two identified by XRD) are sometimes present. The REE-rich minerals synchisite and parisite may occur as interstitial phases (Neumann et al. 1990). Several rare minerals, including some fluorides and niobates, occur in the miarolitic cavities or in the rock proper (Dietrich et al. 1965, Raade 1972, Raade & Haug 1980, Neumann et al. 1990). Locally, the rock has undergone pronounced sub-solidus alteration, resulting in the replacement of pyriboles by oxides (mainly hematite) and quartz ( $\pm$  chlorite,  $\pm$  calcite).

Aplitic (generally alkali feldspar porphyritic, and sometimes quartz porphyritic) and pegmatitic varieties occur in variable, but usually subordinate amounts (Brøgger 1906, Sæther 1962, Hansteen 1988). Both gradational and sharp contacts to nordmarkitic (quartz syenitic) rocks occur locally in the complex. Late, quartz-dominated veins are common in several parts of the ESG. Cross-cutting, pyrite-rich veins occur in variable amounts.

### Miarolitic cavities

Miarolitic cavities are very abundant in the ESG. They occur in all sizes, from microscopic cavities about 0.05 mm in diameter to mineral-lined pockets almost 1 m wide.

### Miarolitic interstices

The smallest cavities are simply interstices with diameters of roughly 0.05 to 1 cm, into which primary magmatic minerals protrude. Generally, only those parts of the minerals which grew freely into the cavities have euhedral crystal faces. Most of the larger cavities are partly filled with quartz, perthitic alkali feldspar ( $\pm$  albite), ægirine and/or alkali amphibole.

### Miarolitic veins and cavities

The larger miaroles are surrounded by transition zones which grade into the host rock. Moving towards the cavity, the texture of the host rock changes gradually from hypidiomorphic to allotriomorphic granular, to a transition zone composed mainly of coarse quartz-perthite graphic intergrowths (Fig. 2a). These zones are usually 1 to 5 cm wide, but may be wider for the large cavities. The earliest

generation of quartz and alkali feldspar in the miaroles grew epitaxially on to quartz and alkali feldspar grains of the transition zone, and are thus direct physical continuations of the crystals found in the host rock.

The physical shapes of the cavities show large variations. At some localities, miaroles which are separated from each other by massive host rock, occur in close proximity to very elongated cavities of highly variable shapes and diameters, which we prefer to call 'miarolitic veins' (Fig. 2b). The miarolitic veins commonly connect two or more cavities, leading to transitional types (see also Raade 1972). The main minerals in the veins are quartz, perthitic alkali feldspar, ægirine and alkali amphibole. Thus, there is no clear distinction between the mineral parageneses of the miaroles and the miarolitic veins. If a distinction is to be made, size seems to be important: the smaller miarolitic cavities are usually physically isolated from each other, while the larger ones are commonly connected by miarolitic veins.

### Aplite - miarolitic veins

Miarolitic veins may occur completely enclosed by an aplitic rock, which in turn is surrounded by the medium- to coarse-grained host rock (Fig. 2c). The transition zone between miarolitic vein and aplitic has a micrographic texture. Because of the similar textures and modes of occurrence, this type of aplitic is regarded as a variety of the transition zones described above.

## Methods of study

### Optical microscopy

A standard petrographic microscope with magnifications up to 500x was used in the study of standard thin-sections and doubly polished fluid inclusion plates, varying in thickness between 0.1 and 1.5 mm. Techniques for fluid inclusion petrography involved the use of one, two and partially crossed polarizers in combination with both orthoscopic and conoscopic light (e.g. Roedder 1984).

### Scanning Electron Microscopy (SEM)

All SEM observations were done at the Institutt for Geologi, Oslo, using a Jeol JSM-840

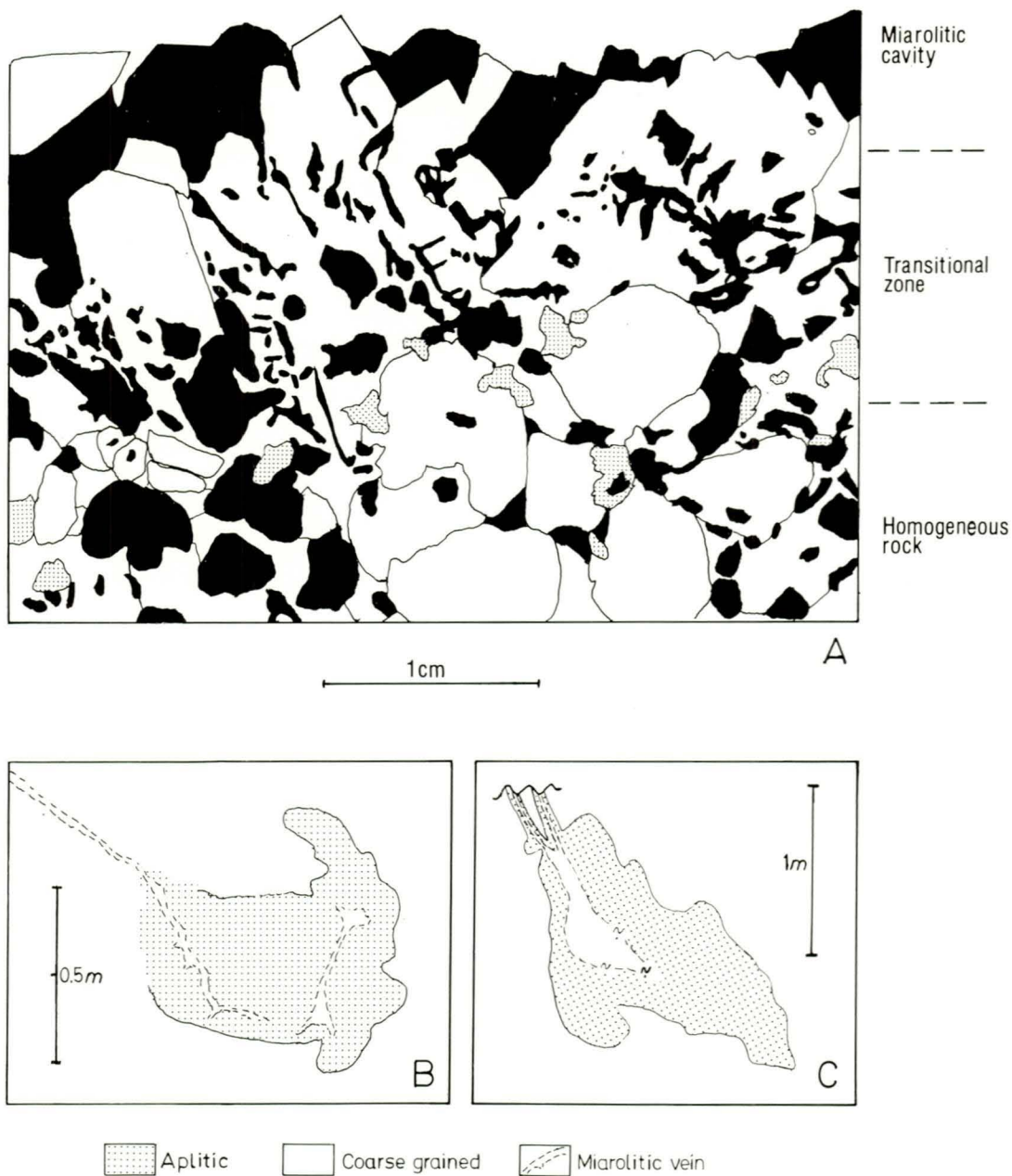


Fig. 2: Rock textures and field relations (Drawn from photographs). A: Micrographic transition zone between massive rock and miarolitic cavity (as seen from a sawn surface). Legend: black- quartz, white- alkali feldspar (perthite); stippled- alkali amphibole. Only the most obvious grain boundaries are drawn in the figure. The bases of the broken, miarolitic crystals (top) are direct continuations of the minerals in the transition zone. B: Miarolitic veins in an aplitic body. One miarolitic vein (top right) connects two small miarolitic cavities within the aplite. The other vein cross-cuts the contact area between aplitic and coarser-grained rock, and gradually fades into the surrounding rock (upper left and centre, respectively). The main minerals in the veins and cavities are alkali feldspar, quartz, alkali amphibole, ægirine and zircon ( sphene), i.e. the main rock-forming minerals. C: Aplite-miarolitic vein association. The miarolitic vein occurs in the aplite, which in turn is surrounded by a coarse-grained rock.

instrument equipped with a Link AN 10000 energy dispersive analyser (EDA) unit. The analyses were performed directly on daughter minerals in opened fluid inclusions. Sample preparation included gentle crushing, mounting on a SEM stub or microscope glass slide, and carbon coating. Due to the irregular sample surfaces, only qualitative analyses were possible. Thus, no absolute element ratios in the daughter minerals are inferred from the SEM analyses in this study. Nearly all ED spectra were recorded using a Be (beryllium) window on the x-ray detector unit. This makes detection of elements lighter than Z=11 (Na) difficult. A few spectra were recorded through a thin plastic foil window, allowing elements down to Z=6 (C) to be detected.

### Laser Raman Microprobe



The laser Raman microprobe analyses were performed at Instituut voor Aardwetenschappen, Vrije Universiteit, Amsterdam, on a Dilor Microdil 28 instrument. In this system, an Ar-laser beam with a wavelength of 514.5 nm is focused inside the inclusion cavity through a microscope. The Raman scattered light is collected at an angle of 180° through the same microscope, and spectra are recorded by a multichannel detector system. Resolution lies in the 1 µm range and is limited by the diameter of the laser beam (Burke & Lustenhouwer 1987).

Optical microscopy, SEM and laser Raman microprobe were used in the identification of daughter minerals in fluid inclusions. For practical reasons, SEM EDA and laser Raman analyses were performed on daughter minerals in different inclusion cavities. Optical properties and morphology were used to ascertain that the same mineral species were analysed with both methods.

### Microthermometry

All microthermometry measurements were performed on Chaixmeca combined cooling and heating stages. One (at Vrije Universiteit, Amsterdam) is cooled by liquid N<sub>2</sub> under pressure; the other (at Mineralogisk-Geologisk Museum, Oslo) uses pre-cooled, gaseous N<sub>2</sub>. Both instruments are calibrated in the T interval +100 to +450°C using various natural and synthetic standards, as described by Roedder (1984).

### SOLID INCLUSIONS

TYPE	CONTENTS
M	Single mineral grains 
MC	Mineral clusters 

### FLUID INCLUSIONS (All types aqueous)

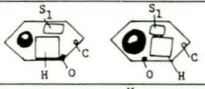
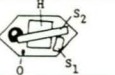
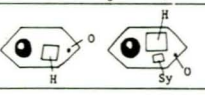
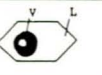
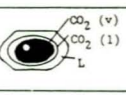
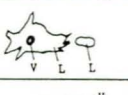

TYPE	MINIMUM DAUGHTER MINERAL ASSEMBLAGE
1A	Halite, one sulphate, calcite, an opaque 
1B	Halite, two sulphates, an opaque 
1C	Halite (±sylvite), an opaque 
CONTENTS / CHARACTERISTICS	
2	H <sub>2</sub> O (l), H <sub>2</sub> O (v), DF > 0.5 
3	H <sub>2</sub> O (l), CO <sub>2</sub> (l), CO <sub>2</sub> (v), DF variable 
4	H <sub>2</sub> O (l), H <sub>2</sub> O (v), irregular, DF (variable) > 0.9 
v	H <sub>2</sub> O (l), H <sub>2</sub> O (v) (±CO <sub>2</sub> (v)), DF < 0.5 

Fig. 3: Types of inclusions found in the ESG. The classification is based on observations at room temperature, and comprises both solid inclusions (which do not contain any optically distinguishable liquid phase) and fluid inclusions (which contain at least one liquid phase). Abbreviations: G - glass (devitrified), V - vapour, L - liquid, O - opaque, H - halite (NaCl), Sy - sylvite (KCl), S<sub>1</sub>, S<sub>2</sub> - sulphates, C - calcite, DF - degree of fill, defined as the volume fraction of the inclusion which is not occupied by the vapour bubble. See text for the identification of solid phases.

For all CO<sub>2</sub> triple point (T<sub>mCO<sub>2</sub></sub>) measurements performed, the reproducibility was found to be better than 0.2°C.

### Electron microprobe

Electron microprobe analyses of various mineral phases included in quartz were obtained

at the Mineralogisk-Geologisk Museum, Oslo, using a Cameca Camebax Microbeam instrument fitted with a Link EDA unit. Due to the small sizes of most of the analysed solids, the results are only regarded as qualitative, and total element ratios are not inferred.

## Definitions of inclusion types

All definitions were made on the basis of observations at room temperature. Each inclusion type is schematically drawn in Fig. 3.

### Solid inclusions

*Type M:* Subhedral to euhedral mineral grains which are completely surrounded by the host quartz. The inclusions contain neither vapour nor liquid.

*Type MC:* Inclusions containing three or more minerals (i.e. mineral clusters) and a vapour bubble, but no visible aqueous fluid.

Both types are commonly between 5 and 50  $\mu\text{m}$  in diameter, although some trapped magmatic minerals (type M) may be considerably larger.

### Fluid inclusions

Unless otherwise stated, the term 'fluid inclusion' is used for inclusions containing at least one liquid phase, with or without daughter minerals.

*Type 1:* Aqueous inclusions containing daughter minerals and having a degree of fill (DF; defined by the expression 1-volume fraction of vapour bubble) of more than 0.5. The possibility that trapped mineral grains were mistaken for true daughter minerals, was precluded by the selection procedure: only species occurring in equal proportions in several adjacent inclusions of each type were considered. Type 1 inclusions are subdivided according to their 'minimum daughter mineral paragenesis' (Fig. 3):

- 1A: Halite ( $\pm$  sylvite), a sulphate, a carbonate, an opaque.
- 1B: Halite, two different sulphates, an opaque.
- 1C: Halite ( $\pm$  sylvite), an opaque.

The occurrence of one or two daughter sulphates are thus diagnostic for the type 1A and 1B inclusions, respectively.

*Type 2:* Aqueous inclusions without daughter minerals and with a DF of more than 0.5.

*Type 3:* Inclusions containing both aqueous

solution and visible amounts of liquid + gaseous  $\text{CO}_2$ .

*Type 4:* Aqueous inclusions with irregular shapes and a DF varying unsystematically between 0.9 and 1.0 in the same trail. They are always secondary and cross-cut all other inclusion textures.

*Type V:* Inclusions with a DF of less than 0.5, i.e. vapour-rich inclusions. They may contain gaseous  $\text{CO}_2$ , but no visually detectable liquid  $\text{CO}_2$ .

## Occurrence and sizes of inclusions

Fluid and solid inclusions in two different types of quartz were treated in this study:

1) Inclusions in rock-forming (magmatic) quartz, both from the equigranular, medium- to coarse-grained rock, and from quartz porphyritic samples.

2) Inclusions in euhedral quartz crystals found in miarolitic veins and cavities.

The sizes of the fluid inclusions are highly variable, also among inclusions of the same type, but usually vary between 2 and 30  $\mu\text{m}$  (diameters) in rock-forming quartz, and between 5 and 75  $\mu\text{m}$  in miarolitic quartz. In miarolitic quartz, fluid inclusions of a given type have similar and generally regular shapes, and negative host crystal shapes are common. In magmatic quartz, the shapes may be highly variable, even among neighbouring inclusions of the same type. They range from completely irregular, through smooth and rounded, to negative crystal shapes.

## Inclusion chronology

Following Roedder (1981), the inclusions were grouped as *primary*, *secondary* and *pseudosecondary* according to their modes of occurrence. Relative ages of the primary and pseudosecondary inclusions in a crystal are seen from their positions relative to crystal growth directions, and their spatial relationships to growth zones where these are present (Fig. 4). The chronology of the secondary inclusions appears from cross-cutting relationships, where inclusions from a younger trail may fill in the cavities from an older trail, and in some cases partially obliterate the trail. Different generations of primary and pseudosecondary inclusions

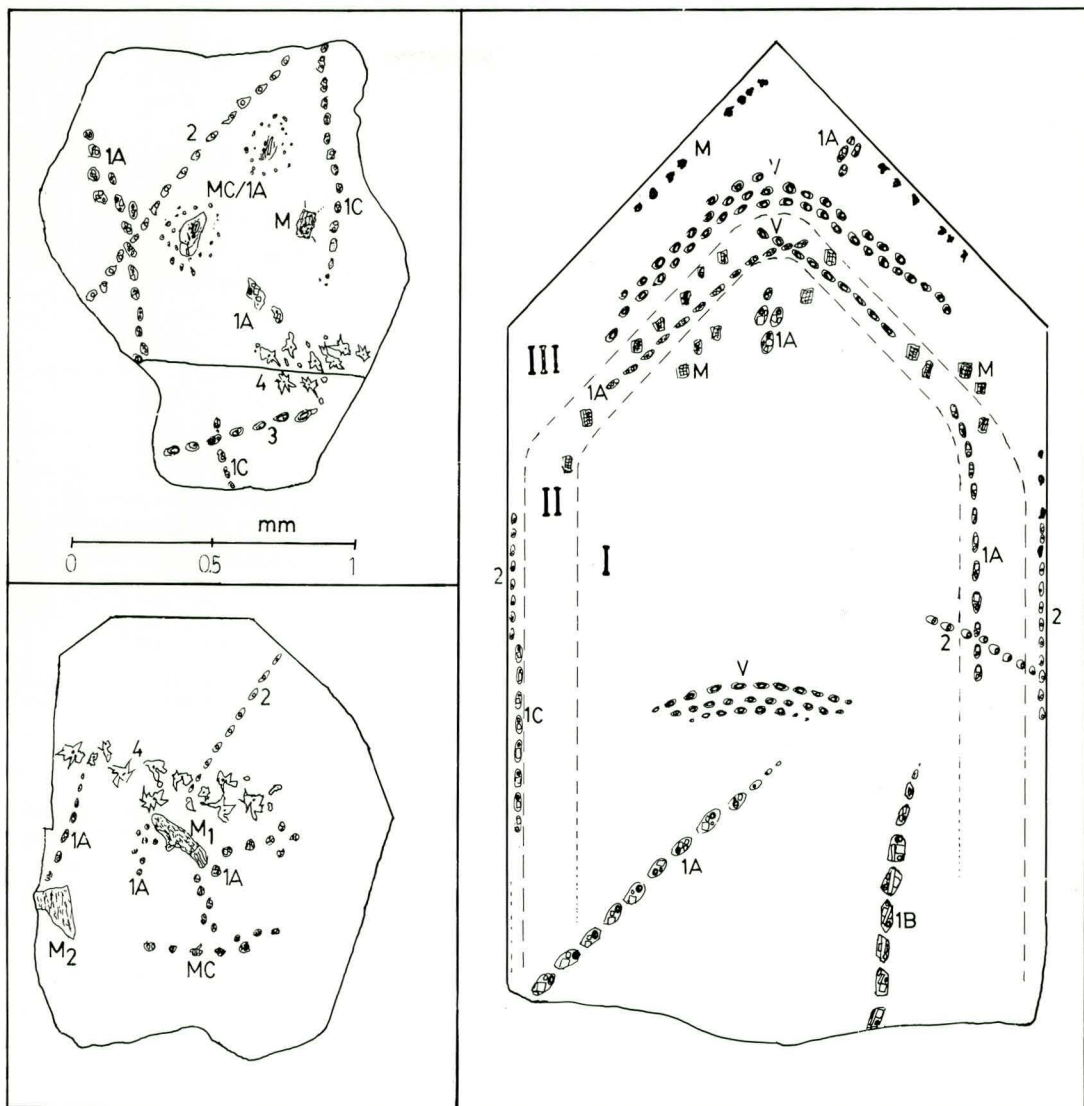


Fig. 4: Inclusion textures shown by simplified sections through three selected samples. A: A rock-forming quartz crystal (from a slightly quartz- and alkali feldspar porphyritic aplite). B and C: Quartz crystals from miarolitic cavities. Note that the inclusion sizes are exaggerated for clarity. The crystal in B is unzoned, while C contains three distinct growth zones, denoted I, II and III, respectively. Crystal diameters are 1.2 mm (A; see scale bar), 6 mm (B) and 6 mm (C), respectively.

ons were not inferred from anhedral, rock-forming quartz grains.

Several types of inclusions occur in each of the quartz crystals studied, but only rarely are *all* types described above found within a single crystal. Thus, the general inclusion chronology was worked out by comparing all available fluid inclusion sections (see Fig. 1 for

sample localities). The general chronology was then compared to detailed observations from each of the sections, and no contradictions were found. One rock-forming and two miarolitic quartz crystals were selected in order to illustrate the inclusion chronology (Fig. 4 a,b and c, Fig. 5).

The quartz grain in Fig. 4a (from the massi-

ve rock) contains primary MC inclusions, surrounded by haloes of primary 1A (or 1B?) inclusions (cf. Fig. 6a). Although it has not been possible to positively identify the daughter minerals in these very small (i.e. < 5 µm diameter) inclusions, only one candidate for a sulphate mineral occurs in each cavity, and they are thus regarded as 1A inclusions. They coexist with a few type V inclusions. Several primary M inclusions occur in the same grain, along with 1A inclusions. Types 1A, 2, 3 and 4 all occur as secondary inclusions; of these, type 4 inclusions are the latest, because they cross-cut all other trails.

A distinction is made between early *primary* and *pseudo-secondary* inclusions in rock-forming and miarolitic quartz and *late primary* inclusions which occur in the outer parts of miarolitic quartz. The crystals in Fig. 4b and c are both from miarolitic cavities.

The crystal in Fig. 4b contains an early primary type M inclusion (an amphibole grain, marked M1). Both 1A and MC inclusions occur in primary groups. Also, a secondary 1A trail occurs in this unzoned crystal. A late primary M inclusion (a feldspar, marked M2) occurs in the lower left part. Several secondary type 1C, 2 and 4 trails, of which type 4 is always the latest, cross-cut the crystal.

The zoned crystal in Fig. 4c contains pseudo-secondary type 1B and type V inclusions along separate cracks in the innermost growth zone

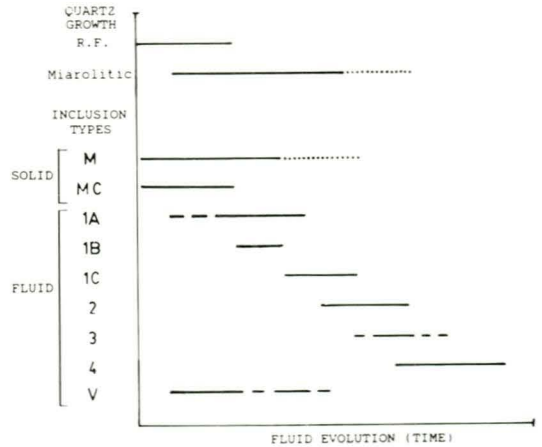


Fig. 5: Inclusion chronology; diagrammatic summary of inclusion textures in the ESG. The horizontal bars represent the relative times of entrapment for each inclusion type. (Note that type V inclusions may coexist with type 1A, 1C and 2 inclusions.) The relative times of formation of the miarolitic and rock-forming (R.F.) quartz is also indicated. Dashed bars mean local variations, while the dotted line for the M inclusions indicates that various mineral species were trapped throughout the growth period for miarolitic quartz. The dotted line extending from the miarolitic quartz growth bar, denotes that many crystals contain late, thin overgrowths (cf. Fig. 4C).

(I), and primary 1A and M (probably feldspar) inclusions in the upper parts of the same zone. A pseudosecondary 1A trail terminates in zone II. Primary and pseudosecondary 1A

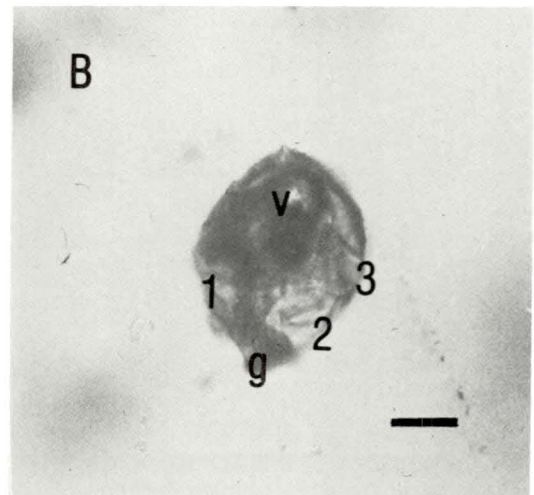
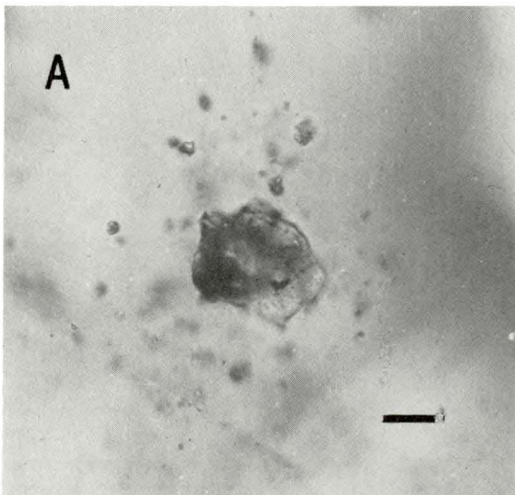


Fig. 6: Primary type MC solid inclusions. The scale bars are 10 µm. A: From rock-forming quartz. The solid inclusion is surrounded (in three dimensions) by type 1A and type V fluid inclusions (cf. the MC/1A inclusion assemblage in Fig. 5A). B: MC inclusions from miarolitic quartz. The inclusions contain at least three solids (1,2,3), a vapour bubble (v) and devitrified glass (g).



and V inclusions occur in separate groups and trails in all growth zones. Intermingled 1A and M inclusions (feldspar grains) occur along the primary growth planes which separate zones I/II and II/III in the upper parts of the crystal. Type M solids (mostly opaques) and type 1C fluid inclusions are found as late primary generations in the outermost growth zone (III). Type 2 inclusions are the latest, occurring along the outermost growth planes and along secondary cracks.

Summing up, only M, MC and 1A ( $\pm$ V) coexist as early, true primary inclusions in both rock-forming and miarolitic quartz. They are thus the earliest inclusions. In some samples, only the larger of the earliest primary/pseudo-secondary fluid inclusions have nucleated a sulphate daughter, and are thus 1A/1C borderline cases (Hansteen 1988). Types M, 1A or 1B occur as later primary or early pseudo-secondary inclusions in rock-forming and miarolitic quartz. Secondary type 1A inclusions are also common. The magmatic quartz may additionally contain some secondary 1B inclusions (not shown in Figs. 4 and 5). Vapour-rich (type V) inclusions occur along pseudo-secondary and secondary cracks, either alone or intermingled with 1A or 1C inclusions. Not all 1A and 1C generations do, however, coexist with V inclusions (partially stippled line for V inclusions in Fig. 5). Type 1C inclusions are either secondary, or late-primary in miarolitic quartz. Type 2 inclusions (which may coexist with type V) are always later than type 1C. The CO<sub>2</sub>-rich type 3 inclusions are later than type 1C, and usually postdate type 2. Type 4 inclusions occur along the latest secondary cracks.

Samples from a majority of the localities do not contain type 1B and 3 inclusions. There is, however, no correlation between the occurrence of the two inclusion types.

## Identification of solid phases

### *Solid inclusions*

Both optical properties and electron microprobe analyses were used for identification purposes.

Early primary and pseudo-secondary solid inclusions comprise the types M and MC, where the M inclusions are trapped mineral grains. The minerals (M) identified are (Table

TABLE 1	
Type M trapped solids	
Alkali feldspar	
Ægirine	
Alkali amphibole	
Apatite	
Sphene	
'Dolomite'	

Table 1: Identified type M solid inclusions (trapped mineral grains).

1): acmitic pyroxene, apatite, alkali amphibole, sphene and alkali feldspar (i.e. the main rock-forming minerals). In addition, a solid inclusion of a mineral from the dolomite group (iron-rich dolomite?) has been identified by its high birefringence and a characteristic Raman line at 1099 cm<sup>-1</sup> (dolomite line at 1099 cm<sup>-1</sup>; White 1974). However, due to the locally high abundance of secondary inclusions, its primary, magmatic origin could not be proven.

Type MC inclusions have only been studied optically. Most MC inclusions contain a vapour bubble, partially devitrified glass (identified according to its optics; semi-isotropic with a brownish shade and a finely speckled appearance), at least one light-coloured mineral grain (tentatively identified as an alkali feldspar on the basis of a low to moderate birefringence and a refractive index (RI) lower than quartz), at least one small opaque and a somewhat larger, dark brown to semi-opaque grain (Fig. 6b). MC inclusions may have somewhat variable contents and phase proportions: some inclusions contain or are attached to elongate, prismatic and moderately birefringent minerals (possibly amphibole or pyroxene). Thus, transitional types between M and MC occur. In MC inclusions that have been cross-cut by later generations of *fluid* inclusions, the glass is very dark (sometimes semi-opaque), and appears coarsely speckled between crossed polarizers. This is interpreted as a sign of devitrification.

Most of the late primary solid inclusions (all are of type M) have a low to moderate birefringence and a RI lower than quartz, and are tentatively assumed to be feldspar. An opaque phase was identified by ED analyses as a Ti-Y-niobate.

### *Fluid inclusions*

*Type 1A inclusions.* All type 1A inclusions contain a halite cube (Table 2, Fig. 7a). This

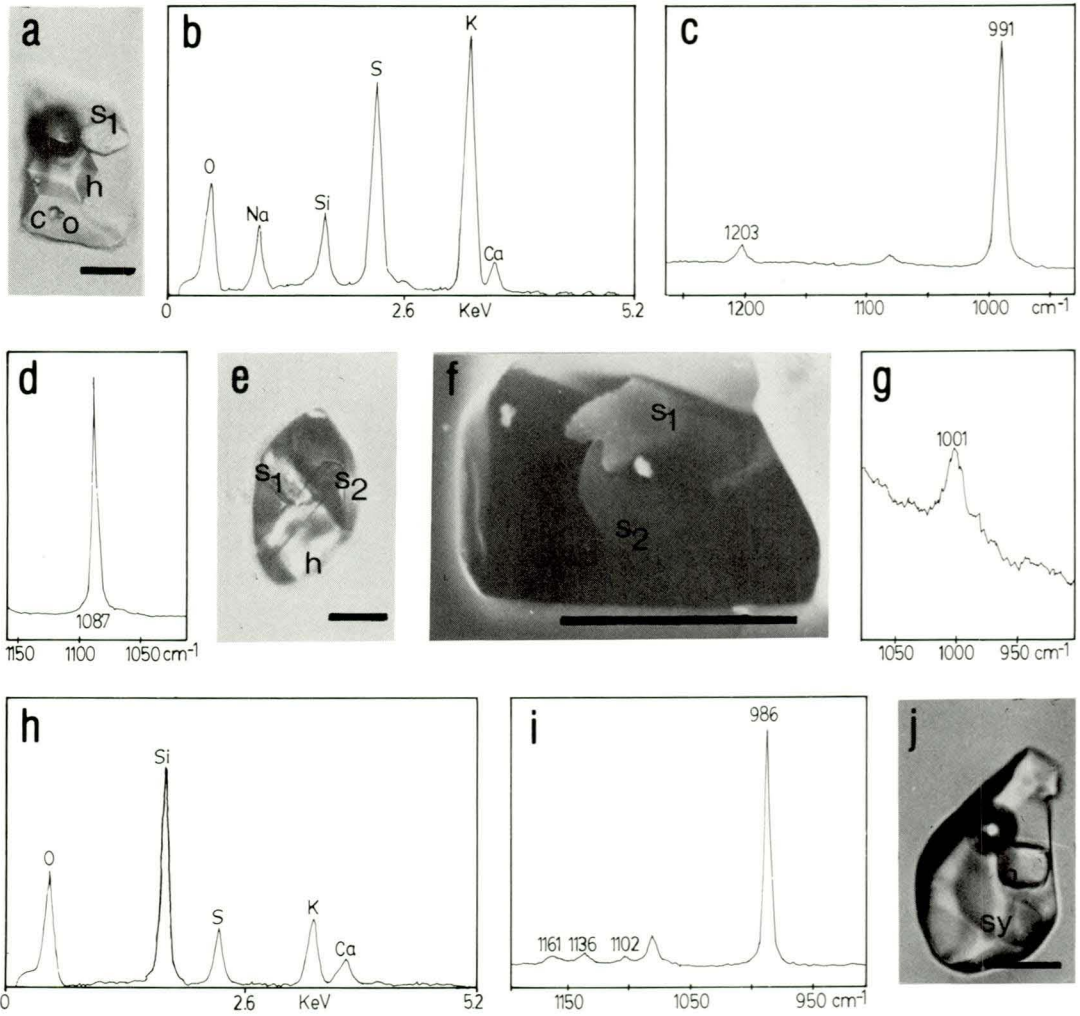


Fig. 7: Identification of daughter minerals in type 1 (i.e. 1A, 1B, 1C) fluid inclusions. All scale bars are 10 μm. A to D cover 1A inclusions, E to I treat 1B inclusions and J, 1C inclusions. A: Photo of 1A inclusion showing halite (h), apththitalite (S1), calcite (c), an opaque (o). B: EDS of S1 (above), containing peaks for Na, S, K (and minor Ca). The Si peaks in all presented EDS originate from the host quartz. C: Raman spectrum of apththitalite. (In the cases where additional Raman lines were used for identification purposes, these are mentioned in the text.) D: Raman spectrum of calcite. E: Photo of 1B inclusion. S2 = görgeyite; other abbreviations as in A. F: SEM image of 1B inclusion, showing apththitalite (S1) and görgeyite (S2). G: Raman spectrum of the S2 grain in E (above); görgeyite. H: EDS of görgeyite, giving lines for S, K, Ca. I: Raman spectrum of barite, as found in some 1B inclusions. J: Photo of 1C inclusion; abbreviations as above.

was identified through energy dispersive spectra (EDS) containing Na and Cl peaks, its shape (in most cases the cube), optical characteristics (isotropic, RI close to that of quartz) and characteristic freezing and heating properties (formation and subsequent incongruent melting of hydro-halite, NaCl·2H<sub>2</sub>O (Roedder 1971)). Sylvite (KCl) is present in some 1A

inclusions. It was identified by its optical properties (isotropic, RI lower than halite), rapid dissolution upon heating (Roedder 1971), inertness upon cooling and in some instances its shape (the cube) which was not, however, used as the sole identification criterion.

Most 1A inclusions contain two small opaques, none of which can be moved by placing

TABLE 2

INCLUSION TYPE	BIREFRINGENCE	EDA	RAMAN (cm <sup>-1</sup> )	IDENTIFICATION
1A	Isotropic	Na, Cl		Halite
	Isotropic	K, Cl		Sylvite
	Moderate	S, Na, K	991 / 1202	Aphthitalite
	Low	K, Al		Potassium fsp.*
	High		1087	Calcite
1B	Opaque	Fe		Magnetite ?
	(Semi)opaque	Ti		TiO <sub>2</sub> ?
	Moderate			Unknown
1C	Isotropic	Na, Cl		Halite
	Moderate	S, Na, K	991 / 1202	Aphthitalite
	Moderate	S, Ca, K	1002 / 625	Görgeyite ?
	High			Calcite ?
	Low		986 / 1136	Barite
1C	Opaque			Mag/Ilm ?
	Isotropic			Halite
	High			Sylvite
1C	Opaque			Calcite ?
				?

\*) Possibly accidentally trapped grains.

Table 2: Daughter minerals identified from type 1 fluid inclusions. (Note that all species do not occur in all inclusion cavities of a given type; cf. Fig. 3 for minimum daughter mineral parageneses). Observations of optical properties were performed on daughter minerals in unopened fluid inclusions. EDA and laser Raman microprobe analyses were done on daughter minerals in different inclusion cavities. The listed wave-numbers are for the two strongest lines only; additional lines are mentioned in the text.

a hand magnet close to the sample (they could, however, be stuck to the inclusion walls). Two different ED spectra, containing peaks for Ti and Fe, were therefore interpreted as a Ti-oxide and magnetite, respectively (Table 2). (Hematite was ruled out because of a lack of reddish colouration.) Calcite was identified in several inclusions by its high birefringence and its characteristic Raman line at 1087 cm<sup>-1</sup> (calcite line at 1088 cm<sup>-1</sup>; White 1974)(Fig. 7d).

By definition, all 1A inclusions contain a sulphate (see above). Optically, it is recognized by its equant or short prismatic shape (Fig. 7a), its moderate birefringence and RI higher than the surrounding brine. Raman spectra recorded from several inclusions contain characteristic sulphate lines at 981 and 991 cm<sup>-1</sup>, or only at 981 to 985 cm<sup>-1</sup> (Fig. 7c), depending on crystal orientations (see also Ross 1974, Bensted 1976, McMillan 1985). Additional lines appear at 1202, 626 to 627, 618 and 451 ± 1 cm<sup>-1</sup>. Ross (1974) reports a Raman spectrum for apthitalite (=glaserite, which forms a series from K<sub>3</sub> Na(SO<sub>4</sub>)<sub>2</sub> to KNa<sub>3</sub> SO<sub>4</sub>), in which the sulphate group 1 line appears at 991 cm<sup>-1</sup>. Additional lines appear at 1190, 1109, 621 and 450 cm<sup>-1</sup>. This is in

good agreement with our data. J. Dubessy (pers. comm. 1987) reports a 996 to 997 cm<sup>-1</sup> 1 line for apthitalite (given as NaK<sub>3</sub>(SO<sub>4</sub>)<sub>2</sub>), which also agrees reasonably well with our data. The occurrence of apthitalite as a daughter mineral in type 1A inclusions was confirmed by several ED spectra, containing lines for Na, K and S (Fig. 7b). Apthitalite has not previously been reported from Norway.

Some 1A inclusions contain potassium feldspar (K-, Al-lines in the EDS; Table 2) which are, however, interpreted as trapped grains. A few 1A inclusions contain fluorite, which was identified by its optical characteristics (isotropic, RI only slightly higher than the surrounding brine; Shepherd et al. (1985) report RIs of 1.376 to 1.395 for saturated brines). Some 1A inclusions contain a small, irregularly shaped and moderately birefringent unknown (Table 2), which was termed S<sub>x</sub>.

It is worth noting that no sulphate minerals were found as solid inclusions. This is further proof that they are true daughter minerals.

*Type 1B inclusions.* Type 1B inclusions also contain halite, which was identified as described above. An opaque is always present. Because of its dark colour, this non-magnetic

mineral is tentatively identified as ilmenite (or magnetite; see above).

The 1B inclusions contain two relatively large daughter minerals in addition to halite (Fig. 7e). One is identified as apthitalite on the basis of laser Raman analyses (see description above), EDS containing Na-, K- and S-lines, and optical characteristics. The other one is usually long prismatic or lath-shaped with a moderate birefringence and RI higher than the surrounding brine (Fig. 7 e and f). The Raman spectra contain a characteristic sulphate 1 line at  $1002\text{ cm}^{-1}$  (Fig. 7g), and additionally a weak, orientation-dependent line at  $625\text{ cm}^{-1}$ . (The reason for the Raman fluorescence which partially covers these spectra, is not known.) EDS give lines for K, Ca and S (Fig. 7h). The only two simple sulphates which fit with the EDA data, are syngenite ( $\text{K}_2\text{Ca}(\text{SO}_4)_2 \cdot \text{H}_2\text{O}$ ) and görgeyite ( $\text{K}_2\text{Ca}_3(\text{SO}_4)_6 \cdot \text{H}_2\text{O}$ ). Several Raman spectra were recorded from a reference sample of görgeyite (donated by G. Niedermayr through G. Raade). The spectra contain either a broad sulphate peak at  $1001\text{ cm}^{-1}$ , or a dual peak at  $999$  to  $1008\text{ cm}^{-1}$  (depending on crystal orientation), and additionally a smaller peak at  $623$  to  $625\text{ cm}^{-1}$ . In some orientations, the reference sample gave weak Raman fluorescence. Due to vastly larger sample size ( $2\text{ mm}$  compared to  $< 10\text{ }\mu\text{m}$ ) and much less signal scatter (caused by optical effects on passing phase boundaries) for the reference sample as compared to the daughter minerals, a much better signal to noise ratio is expected for the former spectra. In considering this, the similarities between the two sets of spectra strongly suggest that the  $\text{S}_2$  daughter mineral is görgeyite. Additionally, Raman spectra of syngenite recorded by J. Dubessy (pers. comm. 1987) contain 1 lines at  $983$  and  $1009\text{ cm}^{-1}$ , which confirms that the sulphate is not syngenite. It is, therefore, indeed assumed to be görgeyite. (Görgeyite has not previously been reported from Norway.)

Barite was identified in some 1B inclusions by Raman analyses (Fig. 7i, Table 2). The spectra contain lines at  $1161$ ,  $1136$ ,  $1102$ ,  $986$ ,  $644$ ,  $614$  and  $452\text{ cm}^{-1}$  (the last one as a shoulder on the  $463\text{ cm}^{-1}$  quartz peak). This is consistent with the barite spectrum reported by Griffith (1970), which contains lines at  $1167$ ,  $1140$ ,  $1083$ ,  $987$ ,  $646$ ,  $630$ ,  $617$ ,  $460$  and  $451\text{ cm}^{-1}$ . No carbonate mineral was identified in the type 1B inclusions, but a small, highly bire-

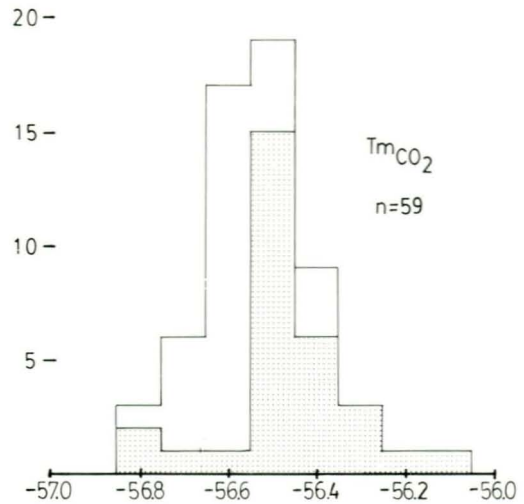


Fig. 8: Frequency histogram showing (triple point) melting temperatures for  $\text{CO}_2$  ( $T_{m\text{CO}_2}$ ;  $+56.6^\circ\text{C}$ , Weast 1984), including type 3 inclusions (shaded), and type V inclusions (white).

fringent grain occurring in some cavities is thought to be calcite.

**Type 1C inclusions.** Halite is the main daughter mineral in type 1C inclusions. Sylvite is commonly present as a small, sometimes rounded cube (Fig. 7j). Both minerals were identified as described above. A small, highly birefringent solid was tentatively identified as calcite (cf. types 1A and 1B above). All 1C inclusions contain a non-magnetic but otherwise unidentified opaque.

### Compositions of inclusion liquids

The liquids in type 1 inclusions (i.e. 1A, 1B, 1C) must be saturated with respect to each of the daughter minerals they contain. Thus, the daughter minerals reflect their chemical compositions. The liquids in type 2, 4 and most type 3 inclusions do not contain daughter minerals, and their chemical compositions cannot be inferred without further analyses.

Microthermometric studies (Hansteen 1988) show that salinities in terms of weight % NaCl equivalents (Clynne & Potter 1977), and final homogenization temperatures of type 2, 4 and V inclusions vary systematically according to their times of entrapment. Type 3 inclusions have highly variable salinities and, in addition, highly variable phase proportions and densities.

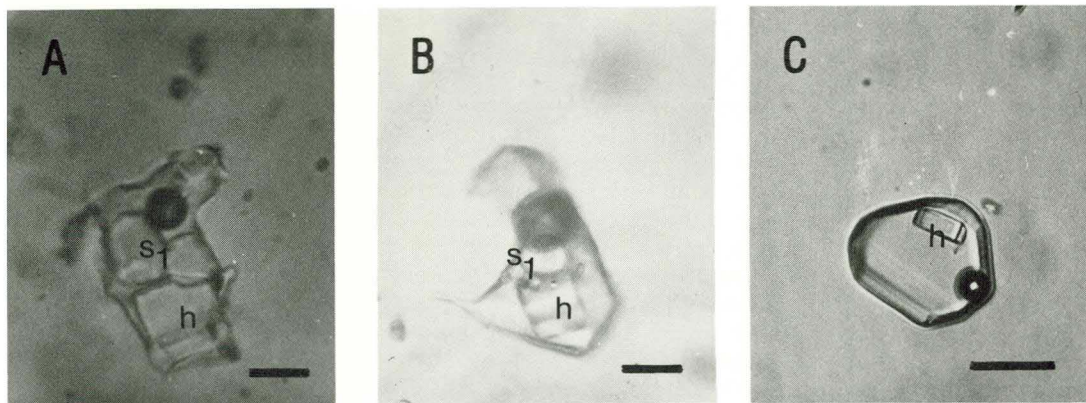


Fig. 9: The gradual change in fluid compositions from early, submagmatic 1A to post-magmatic 1C inclusions. Abbreviations as in Fig. 3; scale bars are 10 µm. A: An early 1A inclusion, dominated by halite and a large aphthitalite grain (S1; in this case a twinned grain). B: Later 1A inclusion, containing only a small aphthitalite grain. C: Type 1C inclusion containing halite, but no sulphate mineral.

Many type V inclusions contain CO<sub>2</sub> vapour (±liquid) at ambient temperatures. The purity of the CO<sub>2</sub> in both type 3 and type V inclusions was checked through TmCO<sub>2</sub> measurements, which are compared to the triple point for CO<sub>2</sub> (-56.6° C; Weast 1984) in Fig. 8. Within the accuracy of the method, the data show that the CO<sub>2</sub> is pure.

TABLE 3

TYPE	Na	K	S	Cl	Ca	(Ba)	H <sub>2</sub> O	n
Magm 1A/1C	11.2	1.7	0.4	18.0	0.1	-	68	6
Magm 1A	21.9	6.6	4.8	29.1	-	-	28	7
Early sub 1B	15.3	4.5	5.0	20.0	1.7	1	42	14
Early sub 1A	17.3	5.6	4.6	21.4	0.1	-	42	5
Early sub 1A	15.9	3.0	2.5	21.9	0.3	-	50	17
Late sub 1A	8.2	1.9	1.6	10.8	0.1	-	74	8

Table 3: Compositions of type 1A and 1B fluid inclusions, calculated from phase proportions of identified daughter minerals and inclusion fluids. All values are in weight %. See text for discussion of results.

## Discussion

### Evolution of magmatic fluids

The earliest generations of fluids in the ESG are represented by primary and pseudosecondary 1A inclusions found in close spatial connection to type MC solid inclusions (Fig. 6a). The latter are interpreted as samples of trapped silicate melt. The earliest 1A (including 1A/1C borderline cases) and coexisting V inclusions were directly derived from a silicate melt during its crystallization, and are thereby magmatic. The pseudosecondary 1B inclusions were trapped early during the formation of miarolitic quartz, and seemingly overlap in time with some 1A inclusions. These slightly later fluids did not coexist with a silicate melt, but as seen from their daughter mineral contents, they were compositionally similar to the magmatic fluids (Table 3). We use the term 'submagmatic fluids' as a descriptive and genetic term for the 1B and strictly non-magmatic 1A and 1A/1C inclusions, and define this as sub-

solidus fluids possessing the chemical characteristics of the magmatic fluids (see also Buddington & Lindsley (1964) for the term 'submagmatic'). It follows from this that the term 'post-magmatic' is used to describe fluids which post-date and do not have the chemical characteristics of the submagmatic fluids. No sharp division exists between magmatic and submagmatic fluids in the ESG.

Based on inclusion petrography, there is a gradual change in fluid regime from 1A to 1C inclusions at many localities. The early submagmatic 1A inclusions contain relatively large sulphate crystals (Fig. 9a), while the the latest 1A inclusions only contain very small grains (Fig. 9b). The later 1C inclusions do not contain any sulphate grains (Fig. 9c). The occurrence of type V inclusions partially coexisting with 1A and 1C inclusions suggests that fluid unmixing occurred during the submagmatic stage (Hansteen 1988).

## Compositions of type 1A and 1B inclusions

The sizes of several 1A and 1B inclusion cavities and their respective daughter minerals were measured optically through a graded micrometer ocular, and their relative volumes calculated through comparison with simple geometrical figures. The volume of the vapour bubble was subtracted from the total volume, and the weight percentages of each identified mineral calculated using the simplifying assumption that the inclusion fluids are pure H<sub>2</sub>O. (Aphthitalite in all inclusions was regarded to be K<sub>2</sub>Na<sub>2</sub>(SO<sub>4</sub>)<sub>2</sub>). Thus, rough estimates of the main element compositions of type 1A and 1B fluids were obtained (Table 3).

Because several inclusions of each type were measured, the unsystematic errors inherent in the method of measurement are consequently likely to be balanced out. The remaining uncertainties are mainly the following:

1) All species dissolved in the brines at room temperature were neglected due to the lack of solubility data in such complex systems. However, data from Linke (1958) and Harris et al. (1979) suggest that the solubilities of e.g. NaCl and KCl at room temperature are drastically lowered (i.e. by up to an order of magnitude) in solutions containing divalent (and polyvalent) cations. Alkali sulphate solubilities are generally of the same order of magnitude as, or lower by an order of magnitude than, those for alkali chlorides (Weast 1976, Møller 1988).

2) Unidentified daughter mineral grains occurring in most large inclusions of each type suggest that additional elements are present.

The above two factors have opposite effects on the calculated main element concentrations, and thus cancel each other to some extent; but the calculated values must still be regarded as rough estimates only.

Sodium and chlorine are by far the most abundant elements in all type 1A and 1B inclusions (as expected from the high halite contents) (Table 3). Calculated values range from 8.2 to 21.9 wt % for Na, and from 10.8 to 29.1 wt % for Cl. Sulphur and potassium contents are lower, and internally comparable within most inclusion groups: they are between 0.4 and 5.0 wt %, and between 1.7 and 6.6 wt %, respectively. The magmatic inclusions show comparatively large variations in the concentra-

tions of all elements listed. This is not unexpected if the inclusions are interpreted as representing different aliquots of fluids given off from a crystallizing silicate melt (Kilinc & Burnham 1972, Holland 1972, Burnham 1979). (A complementary explanation involves concentration through fluid boiling or unmixing; e.g. Roedder 1984). The relative times of formation for the different magmatic fluid inclusions are, however, unknown. If the less saline magmatic inclusions (i.e. 'Magm 1A/1C' in Table 3) are excluded, there is a gradual decrease in all elements listed from the magmatic throughout the submagmatic stage. However, the more saline magmatic inclusions (i.e. 'Magm 1A' in Table 3) and the early submagmatic inclusions, all show comparable Na, K, S and Cl contents. The comparatively high calculated Ca contents of the 1B inclusions are due to the occurrence of görgeyite. The Ba concentration of 1 wt% in the 1B inclusions is somewhat surprising (although this is a maximum value due to the low solubility of barite; Weast 1984).

Except for the higher Ba and Ca contents in the 1B inclusions, the calculated main element contents in the 1B and early submagmatic 1A inclusions are quite similar. The later generations of 1A inclusions have lower concentrations of all listed elements. No estimates of Fe and/or Ti contents in the inclusions were made, because of the uncertain identities of the opaque(s).

## The magmatic and submagmatic stages

The high Na, K, S and Cl concentrations in the early 1A inclusions show that these elements were strongly partitioned into the fluid phase which evolved upon crystallization of the ESG magmas (cf. Gammon et al. 1969, Kilinc & Burnham 1972). This effect was especially pronounced for chlorine, which only occurs in negligible amounts in apatite and amphibole (Neumann et al. 1990), and for sulphur, which occurs in the subordinate amounts of pyrite. Because sulphur mainly dissolves as reduced species (notably HS; Burnham 1979) in aluminosilicate melts, the high sulphate concentrations in the magmatic fluid inclusions indicate comparatively high  $f_{O_2}$  values in these fluids.

Fluorite occurs locally as a magmatic mineral, but no fluorides were found as daughter minerals in the magmatic fluid inclusions. These observations are compatible with theoretical and experimental data, showing that fluorine is partitioned into a silicate melt rather than a coexisting fluid phase (Manning et al. 1984). However, some of the late submagmatic 1A inclusions contain  $\text{CaF}_2$ . The comparatively high abundance of late 1A inclusions suggests that much of the fluorine was leached from the magmatic minerals by circulating fluids at a relatively late stage, i.e. under sub-solidus conditions.

Although the ESG feldspar is roughly mesoperthitic, this study indicates that the magmatic and submagmatic fluids had low K/Na ratios (Table 3; see also Hansteen 1988). This is consistent with experimental work on alkali chloride-alkali feldspar systems (Lagache & Weissbrod 1977). Additionally, ægirine and alkali amphibole protruding into the miarolitic cavities (Dietrich et al. 1965) are compatible with low K/Na ratios in the (magmatic to) submagmatic fluids. As seen from the submagmatic type M feldspar inclusions, the aluminium concentrations in the fluids must have been significant, which is also supported by the occurrence of small, trapped, K-feldspar grains in some 1A inclusions (Table 2). Although the opaque phases in the inclusions have not been positively identified, the occurrence of ægirine and alkali amphibole in the miaroles proves that the fluids contained iron (probably transported as  $\text{FeCl}_2$  complexes; Chou & Eugster 1977, Frantz et al. 1981) in addition to the feldspar components.

The occurrence of barite as a daughter mineral in the sub-solidus 1B inclusions testifies to high Ba transport capabilities in these fluids. However, sub-solidus processes seem not to have altered the Ba contents of the ekerites significantly (Neumann et al. 1990).

### Post-magmatic fluids

The high halite to sylvite volume ratios in the sylvite-bearing 1C inclusions show that relatively low K/Na ratios were maintained under post-magmatic conditions (Fig. 7j). Low K/Na ratios are also supported by the pervasive albite rimming of the rock-forming perthite grains. Apart from in fluid inclusions, no sulphate minerals occur in the ekerite, the most likely reason being that potential species are

water soluble. Some of the sulphur loss during the submagmatic to post-magmatic transition can, however, be accounted for by the occurrence of cross-cutting, pyrite-rich veins and small base metal sulphide deposits, some of which have been mined (Foslie 1925).

The 1C to 2 transition is probably best described as a dilution of the type 1C fluids through mixing with low-salinity meteoric water (Hansteen 1988). Late post-magmatic fluids were responsible for some quartz and feldspar dissolution and redeposition (Andersen et al. 1990).

The carbonic type 3 inclusions have higher  $\text{CO}_2/\text{H}_2\text{O}$  ratios than any other inclusion type in the ESG. These late, carbonic fluids can either have formed from  $\text{CO}_2$ -bearing fluids from deeper, hotter levels in the ESG, or through interaction with external fluids. Likely, external sources for the  $\text{CO}_2$ -rich fluids are either the abundant diabase dykes cross-cutting the complex (mafic melts can dissolve significant quantities of  $\text{CO}_2$ ; Eggler et al. 1974) or local Cambro-Silurian calcareous sediments, as proposed for the nearby Drammen biotite granite by Olsen & Griffin (1984). Such rocks also occur as xenoliths in the ESG.

### Fluid evolution trends

In Fig. 10, qualitative fluid evolution trends are described by the relative proportions of Cl, S and  $\text{H}_2\text{O}$  in each inclusion type, as calculated from daughter mineral proportions (Table 3). Na and K are listed in parentheses because they show strong covariation with Cl and S, respectively. (This is only valid for the 1A and 1B inclusions; no measure of S content has been obtained for the 1C or 2 inclusions). It is important to note, however, that this covariation is a direct result of the methods used to obtain the main element contents. The main contributions of the elements Na and Cl come from halite, while the main contributions of K and S come from apthitalite.

The magmatic inclusions show large variations in S and Cl contents (Table 3). As seen from the very small apthitalite ( $S_1$ ) grains in some of these inclusions, the lower limit probably lies just above the (unknown) saturation level for  $S_1$  in these brines. The highest S/Cl ratios occur in the 1B and early submagmatic 1A inclusions (Fig. 10). The submagmatic 1A

fluids first evolved towards S-poorer compositions while Cl remained fairly constant. Towards the later 1A fluids, both chlorine and sulphur concentrations decreased markedly. The total salinities were lowered throughout.

The 1C inclusions have lower sulphur concentrations than the 1A inclusions. Different halite and sylvite solubilities are therefore expected in these inclusion liquids, and direct comparisons with the data in Table 3 can hardly be made on the basis of similar measurements. Thus, the stippled parts of the trend in Fig. 10 (representing the 1C inclusions), is only inferred from approximate daughter mineral contents.

### Formation of miarolitic veins and cavities

The primary magmatic inclusions (MC, 1A, 1A/1C) occurring in both miarolitic and rock-forming quartz strongly suggest that the miarolitic cavities and veins were formed during solidus or even super-solidus conditions. This is supported by the quartz-alkali feldspar micrographic areas which immediately surround and gradually pass into the miaroles, as the earliest miarolitic minerals are direct physical continuations of mineral grains in these transitional zones (Fig. 2). Judging from the above textures, the miaroles must have formed as fluid-rich pockets in a largely solidified crystalline melt mush, as a direct result of late-magmatic fluid exsolution processes (e.g. Burnham 1979). The occurrence of magmatic minerals such as ægirine, alkali amphibole, perthitic feldspar, sphene and zircon which protrude freely into the cavities (Dietrich et al. 1965), supports this interpretation. Thus, the variable shapes of the miarolitic veins and cavities reflect the shapes of the original fluid-rich pockets. As only type 1A ( $\pm$ A/1C) and 1B fluids occur as primary and pseudosecondary inclusions in miarolitic (and rock-forming) quartz, these must be the fluids responsible for miarole formation.

The transition zones surrounding the larger miaroles resemble the descriptions given for a number of zoned pegmatites (see e.g. Cerný 1982). Also the occurrence of several rare minerals both in the rock proper (mostly REE-minerals; E.-R. Neumann, pers. comm. 1987) and in the miaroles, suggests a fluid evolution which at least locally resembles that of pegmatites.

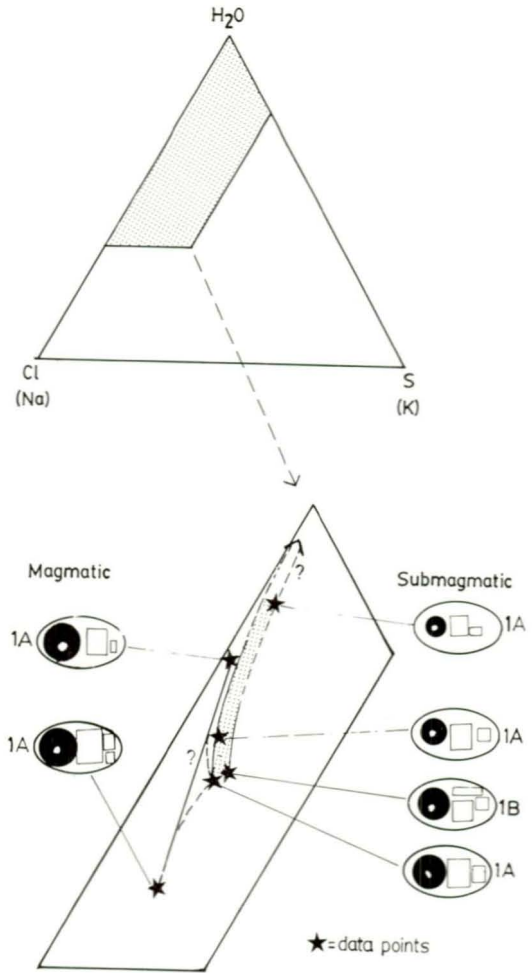


Fig. 10: Fluid evolution trends expressed in terms of Cl-S-H<sub>2</sub>O. The compositions of the 1A and 1B inclusions were calculated from daughter mineral contents, whereas the 1C compositions were only inferred from the daughter minerals present (dashed line trend; see text). All figures are in weight %. Sodium and potassium are indicated in parentheses, because they show covariation with Cl and S, respectively, in the 1A and 1B inclusions.

### Conclusions

Magmatic and submagmatic fluids in the ESG had high contents of Na, K, S and Cl, and are probably best described as hydrosaline melts. Large amounts of these fluids were retained in miarolitic veins and cavities during and after the last stages of magma solidification. The internal fluids retained their chemical characteristics during the submagmatic stage,



resulting in the formation of rare mineral assemblages in the miaroles, comparable to those found in pegmatites (Sæbø 1966, Raade 1972, Raade & Haug 1980). The submagmatic to post-magmatic transition occurred through substantial decreases in sulphate (and probably in alkali chloride) concentrations well after the miaroles were formed. The changes in fluid regime from the magmatic, through the submagmatic to the post-magmatic stage were gradational, owing at least partially to progressive mixing with meteoric water. These conclusions are supported by thorough microthermometric measurements (Hansteen 1988).

### Acknowledgements

Special thanks are due to J. Touret for enthusiastic support during a stay at the Free University in Amsterdam February to April 1986. Funding for this stay, given by the Norwegian Council for Scientific and Technical Research (NTNF) through E.-R. Neumann, is gratefully acknowledged. J. Dubessy kindly provided unpublished Raman reference spectra. Reference specimens of the rare mineral gōrgeyite were donated by G. Niedermayr, through an initiative by G. Raade. Facilities for Laser Raman microprobe analyses were provided by the Free University in Amsterdam and by the WACOM, a working group for analytical chemistry of minerals and rocks; this group is subsidized by the Netherlands Organization for the Advancement of Pure Research (ZWO). J. Touret, E.-R. Neumann, T. Andersen, J. Konnerup-Madsen and an anonymous reviewer improved the manuscript through constructive criticism.

The work reported is part of the programme 'Ores associated with granitic rocks', funded by NTNF as the Norwegian contribution to the EEC research programme on minerals.

## References

- Andersen, T. 1981: En geokjemisk-petrologisk undersøkelse av de intrusive bergartene i Sande Cauldron, Oslofeltet. Unpubl. Cand. Real. thesis, Univ. of Oslo, 321 pp.
- Andersen, T. 1984: Crystallization history of a Permian composite monzonite-alkali syenite pluton in the Sande cauldron, Oslo rift, southern Norway. *Lithos* 17, 153–170.
- Andersen, T., Rankin, A.H. & Hansteen, T.H. 1990: Melt-mineral-fluid interaction in peralkaline silicic intrusions in the Oslo rift, SE Norway. III. Alkali geothermometry based on bulk fluid inclusion content. *Nor. Geol. Unders. Bull.* 417, 33–40.
- Barth, T.F.W. 1945: Studies of the igneous rock complex of the Oslo Region. II. Systematic petrography of the plutonic rocks. *Skr. Nor. Vitensk. Akad. Oslo I.* 1944, 9, 1–104.
- Bansted, J. 1976: Uses of Raman spectroscopy in cement chemistry. *J. Am. Ceram. Soc.* 59, 140–143.
- Brøgger, W.C. 1890: Die Mineralen der Syenitpegmatitgange der sud-norwegischen Augit- und Nephelinsyenite. *Zeitschr. Kryst. und Mineral.* 16, 1–663.
- Brøgger, W.C. 1906: Eine sammlung der wichtigsten Typen der Eruptivgesteine des Kristianiagebietes. *Nyt Mag. Naturvidensk.* 44 115–144.
- Brøgger, W.C. & Schetelig, J. 1926: Rektangelkart Kongsberg (1:100 000), *Nor. geol. unders.*
- Buddington, A.F. & Lindsley, D.H. 1964: Iron-titanium oxide minerals and synthetic equivalents. *J. Petrol.* 5, 310–357.
- Burke, E.A.J. & Lustenhouwer, W.J. 1987: The application of a multichannel laser Raman microprobe (Microdil 28) to the analyses of fluid inclusions. *Chem. Geol.* 61, 11–17.
- Burnham, C.W. 1979: Magmas and Hydrothermal Fluids. In Barnes, H.L. (ed.) *Geochemistry of hydrothermal ore deposits*, sec. edit. J. Wiley & Sons, New York, 71–136.
- Cerný, P. 1982: Anatomy and classification of granitic pegmatites. In P. Cerný (ed.), *Short Course in Granitic Pegmatites in Science and Industry*, short course handbook vol 8, Mineralogical Association of Canada, 1–39.
- Chou, I. & Eugster, H.P. 1977: Solubility of magnetite in supercritical chloride solutions. *Am. J. Sci.* 272, 1296–1314.
- Clyne, M.A. & Potter, R.W. 1977: Freezing point depression of synthetic brines (abstr.). *Geol. Soc. Am. Abstr. Programs* 10, 381.
- Dietrich, R.V., Heier, K.S. & Taylor, S.R. 1965: Studies on the igneous rock complex of the Oslo Region. XX. Petrology and geochemistry of ekerite. *Skr. Nor. Vidensk.-Akad. Oslo. I. Ny ser.* 19, 1–31.
- Eggler, D.H., Mysen, B.O. & Seitz, M.G. 1974: The solubility of CO<sub>2</sub> in silicate liquids and crystals. *Carn. Inst. Wash. Yb.* 73, 226–228.
- Foslie, S. 1925: Syd-norges gruber og malmforekomster. *Nor. geol. unders.* 126 pp.
- Frantz, J.D., Popp, R.K. & Bockr, N.Z. 1981: Mineral-solution equilibria, V. Solubilities of rock-forming minerals in supercritical fluids. *Geochim. Cosmochim. Acta* 45, 69–77.
- Gammon, J.B., Borcsik, M. & Holland, H.D. 1969: Potassium-sodium ratios in aqueous solutions and coexisting silicate melts. *Science* 163, 179–181.
- Gilson, T.R. & Hendra, P.J. 1970: *Laser Raman Spectroscopy*. Wiley Interscience.
- Hansteen, T.H. 1988: Cooling history of the Eikeren-Skrim peralkaline granite complex, the Oslo region, Norway. Evidence from fluid inclusions and mineralogy. Unpubl. Cand. Scient. thesis, Min.-Geol. Museum, Univ. of Oslo, 244pp.
- Harris, H.J.H., Cartwright, K. & Torii, T. 1979: Dynamic chemical equilibrium in a polar desert pond: a sensitive index of meteorological cycles. *Science* 204, 301–303. (See also correction in *Science* 204, 909.)
- Heier, K.S. & Compston, W. 1969: Rb-Sr studies of the plutonic rocks of the Oslo region. *Lithos* 2, 133–145.
- Kilinc, I.A. & Burnham, C.W. 1972: Partitioning of chloride between a silicate melt and coexisting aqueous phase from 2 to 8 kilobars. *Econ Geol.* 67, 231–235.
- Lagache, M. & Weissbrod, A. 1977: The System: Two Alkali Feldspars-KCl-NaCl-H<sub>2</sub>O at Moderate to High temperatures and Low Pressures. *Contrib. Mineral. Petrol.* 62, 77–101.
- Leake, B.E. 1978: Nomenclature of amphiboles. (For Subcommittee on Amphiboles, I.M.A.) *Min. Mag.* 42, 533–563.
- Linko, W.F. 1958: *Solubilities of Inorganic and Metal-Organic Compounds*, Vol. 1, 4th edn. D. Van Nostrand Co., Princeton, NJ, 1487 pp.
- Manning, D.A.C., Martin, J.S., Pichavant, M. & Henderson, C.M.B. 1984: The effect of F, B and Li on melt structure.

- res in the granite system: Different mechanisms? In C.M.B. Henderson (ed.), *Natural Environment Research Council: Progress in experimental Petrology. Sixth progress report of research supported by NERC 1981-1984*, 36-41.
- McMillan, P. 1985: Vibrational spectroscopy in the mineral sciences. In S.W. Kieffer & A. Navrotsky (eds.) *Microscopic to macroscopic, Atomic environments to mineral thermodynamics. Rev. Min.* 14.
- Neumann, E.-R. 1974: The distribution of Mn<sup>2+</sup> and Fe<sup>2+</sup> between ilmenites and magnetites in igneous rocks. *Am. J. Sci.* 274, 1074-1088.
- Neumann, E.-R. 1976: Compositional relations among pyroxenes, amphiboles and other mafic phases in the Oslo Region plutonic rocks. *Lithos* 9, 85-109.
- Neumann, E.-R., Brunfelt, A.O. & Finstad, K.G. 1977: Rare earth elements in some igneous rocks in the Oslo rift, Norway. *Lithos* 10, 311-319.
- Neumann, E.-R., Tilton, G.R. & Tuen, E. 1988: Sr, Nd and Pb isotope geochemistry of the Oslo rift igneous province, southeast Norway. *Geochim. Cosmochim. Acta* 52, 1997-2007.
- Neumann, E.-R., Andersen, T. & Hansteen, T.H. 1990: Melt-mineral-fluid interaction in peralkaline silicic intrusions in the Oslo rift, SE Norway. 1. Geochemistry of the Eikeren ekerite. *Nor. geol. unders.* 417, 1-13.
- Oftedahl, C. 1948: Studies on the igneous rock complex of the Oslo Region, IX. The feldspars. *Skr. Nor. Vidensk. Akad. I.* 1948, 3, 71 pp.
- Olsen, K.I. & Griffin, W.L. 1984: Fluid inclusion studies of the Drammen Granite, Oslo Paleorift, Norway. 1. Microthermometry. *Contrib. Mineral. Petrol.* 87, 1-14.
- Orville, P.M. 1963: Alkali ion exchange between vapor and feldspar phases. *Am. J. Sci.* 261, 201-237
- Raade, G. 1972: Mineralogy of the miarolitic cavities in the Plutonic Rocks of the Oslo Region, Norway. *Mineral. Record* 3, 1, 7-11.
- Raade, G. 1973: Distribution of radioactive elements in the plutonic rocks of the Oslo Region. Unpubl. Cand. Real. thesis, Min.-Geol. Museum, Univ. of Oslo, Norway. 162 pp.
- Raade, G. 1978: Distribution of Th, U, K in the plutonic rocks of the Oslo region, Norway. In Neumann, E.-R. and Ramberg, I.B. (eds), *Petrology and geochemistry of continental rifts. NATO ASI series C*, v. 136, D. Reidel. 185-192.
- Raade, G. & Haug, J. 1980: Rare Fluorides from a soda granite in the Oslo Region, Norway. *Mineral. Record* 11, 3, 83-91.
- Ramberg, I.B. 1976: Gravity interpretation of the Oslo Graben and Associated Igneous Rocks. *Nor. geol. unders.* 325, 194pp.
- Rasmussen, E., Neumann, E.-R., Andersen, T., Sundvoll, B., Fjerdingsstad, V. & Stabel, A. 1988: Petrogenetic processes associated with intermediate and silicic magmatism in the Oslo rift, south-east Norway. *Min. Mag.* 52, 293-307.
- Roedder, E. 1971: Fluid inclusion studies on the porphyry-type ore deposits at Bingham (Utah), Butte (Montana) and Climax (Colorado). *Econ. Geol.* 66, 98-120.
- Roedder, E. 1981: Origin of fluid inclusions and changes that occur after trapping. In L.S. Hollister and M.L. Crawford (eds.) *Short Course in Fluid Inclusions: Applications to petrology*, short course handbook vol. 6, Mineralogical Association of Canada, 101-137.
- Roedder, E. 1984: Fluid inclusions. *Rev. Mineral.* 12, 644 pp.
- Ross, S.D. 1974: Sulphates and other oxy-anions of Group VI. In Farmer, V.C. (ed.) *The Infrared spectra of minerals. Min. Soc. Monograph* 4, 423-444.
- Shepherd, T., Rankin, A.H. & Alderton, D.H.M. 1985: A practical guide to fluid inclusions studies. Blackie & Son Limited, London, 239 pp.
- Sundvoll, B. 1978: Rb/Sr-relationship in the Oslo igneous rocks. In Neumann, E.-R. and Ramberg, I.B. (eds), *Petrology and geochemistry of continental rifts. NATO ASI series C*, v. 136, D. Reidel. 181-184.
- Sæbø, P.C. 1966: A short comment on some Norwegian mineral deposits within the Igneous Rock Complex of the Oslo Region. *Nor. Geol. Tidsskr.* 46, 260-261.
- Sæther, E. 1962: Studies on the igneous rock complex of the Oslo region, XVIII. General investigations of the igneous rocks in the area north of Oslo. *Skr. Nor. Vidensk. Akad. Oslo I. Ny ser.* 1, 184 pp.
- Weast, R.C. 1976: *Handbook of chemistry and physics.* CRC press, Cleveland, Ohio.
- White, W.B. 1974: The carbonate minerals. In Farmer, V.C. (ed.) *The Infrared spectra of minerals. Min. Soc. Monograph* 4, 227-284.